



Susceptibility of rabbits to SARS-CoV-2

Anna Z. Mykytyn , Mart M. Lamers , Nisreen M. A. Okba , Tim I. Breugem ,
Debby Schipper , Petra B. van den Doel , Peter van Run , Geert van
Amerongen , Leon de Waal , Marion P. G. Koopmans , Koert J. Stittelaar ,
Judith M. A. van den Brand & Bart L. Haagmans

To cite this article: Anna Z. Mykytyn , Mart M. Lamers , Nisreen M. A. Okba , Tim I. Breugem ,
Debby Schipper , Petra B. van den Doel , Peter van Run , Geert van Amerongen , Leon de Waal ,
Marion P. G. Koopmans , Koert J. Stittelaar , Judith M. A. van den Brand & Bart L. Haagmans
(2021) Susceptibility of rabbits to SARS-CoV-2, Emerging Microbes & Infections, 10:1, 1-7, DOI:
[10.1080/22221751.2020.1868951](https://doi.org/10.1080/22221751.2020.1868951)

To link to this article: <https://doi.org/10.1080/22221751.2020.1868951>



© 2021 The Author(s). Published by Informa UK Limited, trading as Taylor & Francis Group



[View supplementary material](#)



Published online: 17 Jan 2021.



[Submit your article to this journal](#)



Article views: 1078















[View related articles](#)



[View Crossmark data](#)

Susceptibility of rabbits to SARS-CoV-2¹

Anna Z. Mykytyn ^a, Mart M. Lamers ^a, Nisreen M. A. Okba ^a, Tim I. Breugem ^a, Debby Schipper ^a, Petra B. van den Doel ^a, Peter van Run ^a, Geert van Amerongen^b, Leon de Waal ^b, Marion P. G. Koopmans ^a, Koert J. Stittelaar ^b, Judith M. A. van den Brand ^c and Bart L. Haagmans ^a

^aViroscience department, Erasmus Medical Center, Rotterdam, the Netherlands; ^bViroclinics Biosciences B.V., Viroclinics Xplore, Schaijk, the Netherlands; ^cDivision of Infectious Diseases and Immunology, Department of Biomolecular Health Sciences, Faculty of Veterinary Medicine, Utrecht University, Utrecht, the Netherlands

ABSTRACT

Transmission of severe acute respiratory coronavirus-2 (SARS-CoV-2) between livestock and humans is a potential public health concern. We demonstrate the susceptibility of rabbits to SARS-CoV-2, which excrete infectious virus from the nose and throat upon experimental inoculation. Therefore, investigations on the presence of SARS-CoV-2 in farmed rabbits should be considered.

ARTICLE HISTORY Received 30 October 2020; Revised 21 December 2020; Accepted 21 December 2020

KEYWORDS Rabbit; SARS-CoV-2; COVID-19; coronavirus; susceptibility; transmission

Introduction

Severe acute respiratory syndrome coronavirus 2 (SARS-CoV-2) caused a pandemic only months after its discovery in December 2019 [1]. Slowing down its spread requires a full understanding of transmission routes, including those from humans to animals and vice versa. In experimental settings, non-human primates, ferrets, cats, dogs, deer mice and hamsters have been found to be susceptible to SARS-CoV-2 infection [2–6]. Moreover, ferrets, cats, deer mice and hamsters were able to transmit the virus via the air [2,4,5,6,7]. In domestic settings, both dogs and cats have been found to carry the virus, displaying very mild to more severe symptoms, respectively [7]. Recently, SARS-CoV-2 has been isolated from mink at multiple Dutch farms. Workers at those farms carried viruses that were highly similar to the viruses detected in mink and phylogenetic analyses supported transmission from mink to workers [8]. Thus, measures to control the spread of SARS-CoV-2 should also include preventing spill-over into potential reservoirs, especially since infectious agents can spread rapidly in livestock due to the high densities at which some animals are kept. Given the fact that rabbits are commonly farmed worldwide, we investigated the susceptibility of rabbits to SARS-CoV-2.

Materials and methods

Expression plasmids and cloning

Plasmids in pcDNA3.1 encoding *Homo sapien* angiotensin converting enzyme 2 (ACE2) (OHu20260),

Oryctolagus Cuniculus ACE2 (Clone ID OOb21562D), *Rhinolophus sinicus* ACE2 (ORh96277) and *Hipposideros armiger* ACE2 (Clone ID OHi02685) were ordered from GenScript. Codon-optimized cDNA encoding SARS-CoV-2 S glycoprotein (isolate Wuhan-Hu-1) with a C-terminal 19 amino acid deletion was synthesized and cloned into pCAGSS in between the EcoRI and BglII sites. pVSV-eGFP-dG (#31842), pMD2.G (#12259), pCAG-VSV-P (#64088), pCAG-VSV-L (#64085), pCAG-VSV-N (#64087) and pCAGGS-T7Opt (#65974) were ordered from Addgene. S expressing pCAGGS vectors were used for the production of pseudoviruses, as described below.


Cell lines

HEK-293 T cells were maintained in Dulbecco's Modified Eagle's Medium (DMEM, Gibco) supplemented with 10% foetal bovine serum (FBS), 1X non-essential amino acids (Lonza), 1 mM sodium pyruvate (Gibco), 2 mM L-glutamine (Lonza), 100 µg/mL streptomycin (Lonza) and 100 U/mL penicillin. Cos-7, Vero, and VeroE6 cells were maintained in DMEM supplemented with 10% FBS, 1.5 mg/mL sodium bicarbonate (Lonza), 10 mM HEPES (Lonza), 2 mM L-glutamine, 100 µg/mL streptomycin and 100 U/mL penicillin. All cell lines were maintained at 37°C in a 5% CO₂ humidified incubator.

VSV delta G rescue

The protocol for VSV-G pseudovirus rescue was adapted from Whelan and colleagues [9]. Briefly, a

CONTACT Bart L. Haagmans  b.haagmans@erasmusmc.nl

 Supplemental data for this article can be accessed at <https://doi.org/10.1080/22221751.2020.1868951>

© 2021 The Author(s). Published by Informa UK Limited, trading as Taylor & Francis Group

This is an Open Access article distributed under the terms of the Creative Commons Attribution License (<http://creativecommons.org/licenses/by/4.0/>), which permits unrestricted use, distribution, and reproduction in any medium, provided the original work is properly cited.

70% confluent 10 cm dish of HEK-293 T cells was transfected with 10 µg pVSV-eGFP-ΔG, 2 µg pCAG-VSV-N (nucleocapsid), 2 µg pCAG-VSV-L (polymerase), 2 µg pMD2.G (glycoprotein, VSV-G), 2 µg pCAG-VSV-P (phosphoprotein) and 2 µg pCAGGS-T7Opt (T7 RNA polymerase) using polyethylenimine (PEI) at a ratio of 1:3 (DNA:PEI) in Opti-MEM I (1X) + GlutaMAX. Forty-eight hours post-transfection the supernatant was transferred onto new plates transfected 24 h prior with VSV-G. After a further 48 h, these plates were re-transfected with VSV-G. After 24 h the resulting pseudoviruses were collected, cleared by centrifugation at 2000× g for 5 min, and stored at −80°C. Subsequently, VSV-G pseudovirus batches were produced by infecting VSV-G transfected HEK-293 T cells with VSV-G pseudovirus at a multiplicity of infection of 0.1. Titres were determined by preparing 10-fold serial dilutions in Opti-MEM I (1X) + GlutaMAX. Aliquots of each dilution were added to monolayers of 2×10^4 Vero cells in the same medium in a 96-well plate. Three replicates were performed per pseudovirus stock. Plates were incubated at 37°C overnight and then scanned using an Amersham Typhoon scanner (GE Healthcare). Individual infected cells were quantified using ImageQuant TL software (GE Healthcare). All pseudovirus work was performed in a Class II Biosafety Cabinet under biosafety level 2 (BSL-2) conditions at Erasmus Medical Center.

Coronavirus S pseudovirus production

For the production of SARS-CoV-2 S pseudovirus, HEK-293 T cells were transfected with 10 µg S expression plasmids. Twenty-four hours post-transfection, the medium was replaced for Opti-MEM I (1X) + GlutaMAX, and cells were infected at an MOI of 1 with VSV-G pseudovirus. Two hours post-infection, cells were washed three times with OptiMEM and replaced with medium containing anti-VSV-G neutralizing antibody (clone 8G5F11; Absolute Antibody) at a dilution of 1:50,000 to block remaining VSV-G pseudovirus. The supernatant was collected after 24 h, cleared by centrifugation at 2000× g for 5 min and stored at 4°C until use within 7 days. SARS-CoV-2 pseudovirus was titrated on VeroE6 cells as described above.

Virus stock

SARS-CoV-2 (isolate BetaCoV/Munich/BavPat1/2020; European Virus Archive Global #026V-03883; kindly provided by Dr. C. Drosten) was propagated on Vero E6 (ATCC® CRL 1586™) cells in OptiMEM I (1X) + GlutaMAX (Gibco), supplemented with penicillin (100 IU/mL) and streptomycin (100 IU/mL) at 37°C in a humidified CO₂ incubator. Stocks were produced

by infecting Vero E6 cells at a MOI of 0.01 and incubating the cells for 72 h. The culture supernatant was cleared by centrifugation and stored in aliquots at −80°C. Stock titres were determined by titration on VeroE6 cells. The tissue culture infectious dose 50 (TCID₅₀) was calculated according to the method of Spearman & Kärber [10]. All work with infectious SARS-CoV-2 was performed in a Class II Biosafety Cabinet under BSL-3 conditions at Erasmus Medical Center.

Pseudovirus and live virus infection in vitro

Cos-7 cells plated at 70% density in a 24 well format were transfected 24 h after plating by dropwise addition of 500 ng ACE2 expression plasmids using a PEI ratio of 1:3 (DNA:PEI) in Opti-MEM I (1X) + GlutaMAX. After 24 h, cells were washed twice and replaced with fresh Opti-MEM I (1X) + GlutaMAX prior to pseudovirus or live virus infection. Pseudovirus transduction was performed by infecting plates with 10^3 VeroE6 titrated particles per well. Plates were incubated for 16 h at 37°C before quantifying GFP-positive cells using an Amersham Typhoon scanner and ImageQuant TL software. Authentic virus infection was performed by adding 10^4 TCID₅₀ SARS-CoV-2 per well and incubating plates for 8 h at 37°C. After incubation, cells were formalin fixed, permeabilized with 70% ethanol and stained with 1:1000 mouse anti-SARS nucleoprotein (Sino Biological, 40143-MM05) and 1:1000 rabbit anti-human ACE2 (Abcam), followed by 1:1000 goat anti-rabbit Alexa-Fluor 594, 1:1000 goat anti-mouse Alexa-Fluor 488, and 1:1000 TO-PRO3 (Thermo Fisher) to stain nuclei. Quantification of virus-infected cells was performed using an Amersham Typhoon scanner and ImageQuant TL software as described above, while confocal imaging was performed on a LSM700 confocal microscope using ZEN software (Zeiss).

In vivo study design

Animal experiments were approved and performed according to the guidelines from the Institutional Animal Welfare Committee (AVD277002015283-WP04). The studies were performed under biosafety level 3 (BSL3) conditions. Three-month-old female New Zealand White rabbits (*Oryctolagus cuniculus*), specific pathogen free, and seronegative for SARS-CoV-2 were divided into four groups of three animals. Animals were inoculated under ketamine-medetomidine anaesthesia antagonized using atipamezole intranasally with 1 mL SARS-CoV-2 diluted in PBS (0.5 mL per nostril). Three groups were infected intranasally with respectively 10^4 , 10^5 or 10^6 TCID₅₀ SARS-CoV-2, swabbed daily under the above-described anaesthesia and monitored for clinical signs of infection, including weight

loss and respiratory symptoms, until four days post infection. An additional three animals were infected with 10^6 TCID₅₀ SARS-CoV-2 and monitored for 21 days post infection. Animals monitored for four days were swabbed from the nose, throat, and rectum daily before being sacrificed for pathology on day 4 post infection. Lung and nasal turbinate homogenates were prepared and diluted as approximately 0.2 grams/mL prior to freezing. The remaining three 10^6 TCID₅₀ infected animals were followed until 21 days post infection with swabs taken on days zero to seven, then on days nine, 11, 14 and 21 post infection. In addition, on day 21 serum was collected from these animals for serological testing by drawing blood via the ear under the above-described anaesthesia. All samples were stored at -80°C until further quantification.

Plaque reduction neutralization test 50 (PRNT₅₀)

Serum samples were tested for their neutralization capacity against SARS-CoV-2 as described before [11]. Heat-inactivated (56°C for 30 min) samples were 2-fold serially diluted in Dulbecco modified Eagle medium supplemented with NaHCO_3 , HEPES buffer, penicillin, streptomycin, and 1% foetal bovine serum, starting at a dilution of 1:10 in 50 μL . Fifty μL virus suspension (~ 400 plaque-forming units) was added to each well and incubated at 37°C for 1 h before transferring to VeroE6 cells. After incubation cells were washed and supplemented with medium, followed by an 8 h incubation. After incubation, the cells were fixed with 4% formaldehyde/phosphate-buffered saline (PBS) and stained with polyclonal rabbit anti-SARS-CoV antibody (Sino Biological, 40143-T62), followed by a secondary peroxidase-labeled goat anti-rabbit IgG (Dako). The signal was developed by using a precipitate forming 3,3',5,5' tetramethylbenzidine substrate (True Blue; Kirkegaard and Perry Laboratories) and the number of infected cells per well was quantified using an ImmunoSpot Image Analyzer (CTL Europe GmbH). The serum neutralization titre is the reciprocal of the highest dilution resulting in an infection reduction of $>50\%$ (PRNT₅₀). A titre >20 was considered positive.

RNA extraction and qRT-PCR

Swabs, lung homogenates and nasal turbinate homogenates were thawed and centrifuged at $2000\times g$ for 5 min. Sixty μL supernatant was lysed in 90 μL MagnaPure LC Lysis buffer (Roche) at room temperature for 10 min. RNA was extracted by incubating samples with 50 μL Agencourt AMPure XP beads (Beckman Coulter) for 15 min at room temperature, washing beads twice with 70% ethanol on a DynaMag-96 magnet (Invitrogen) and eluting in 30 μL ultrapure water.

RNA copies per mL were determined by qRT-PCR using primers targeting the E gene [12] and compared to a counted RNA standard curve.

Immunohistochemistry

Semiquantitative assessment of SARS-CoV-2 viral antigen expression in the lungs was performed as reported for SARS-CoV earlier [13] with a few amendments: for the alveoli, 25 arbitrarily chosen, $20\times$ objective fields of lung parenchyma in each lung section were examined by light microscopy for the presence of SARS-CoV-2 nucleoprotein, without the knowledge of the allocation of the animals. The cumulative scores for each animal were presented as number of positive fields per 100 fields. For the bronchi and bronchioles, the percentage of positively staining bronchial and bronchiolar epithelium was estimated on every slide and the average of the four slides was taken to provide the score per animal. For the trachea and nose, the percentage of positively staining epithelium was estimated on every slide.

Results

Rabbit ACE2-mediated SARS-CoV-2 infection

ACE2 dictates the host range for SARS coronaviruses [13], because it engages the viral spike (S) glycoprotein for cell attachment and fusion of the viral and host membranes [14]. Contact residues of human and rabbit ACE2 critical for binding S are relatively well conserved [15]. We overexpressed ACE2 from different species on a receptor-deficient cell line followed by SARS-CoV-2 pseudovirus or authentic virus infection. Successful infection of both SARS-CoV-2 pseudovirus and authentic virus was observed for human, rabbit and the Chinese horseshoe bat (*Rhinolophus sinicus*) ACE2 (Figure 1 (A,B)). The ACE2 from a distantly related bat, the great roundleaf bat (*Hipposideros armiger*), did not support infection and served as a negative control. Transfection of rabbit ACE2 rendered cells susceptible to SARS-CoV-2 infection demonstrated by a clear overlap between infection and ACE2 expression (Figure 1(C)).

Susceptibility of rabbits to SARS-CoV-2 infection

Next, we inoculated three rabbits with 10^6 TCID₅₀ SARS-CoV-2 for a 21 d follow up. None of the inoculated animals showed clinical signs of infection. As shown in Figure 2(A), we found viral RNA in the nose for 21, 14 and 11 days post inoculation (p.i.) per animal (mean shedding of 15.33 days, SD =

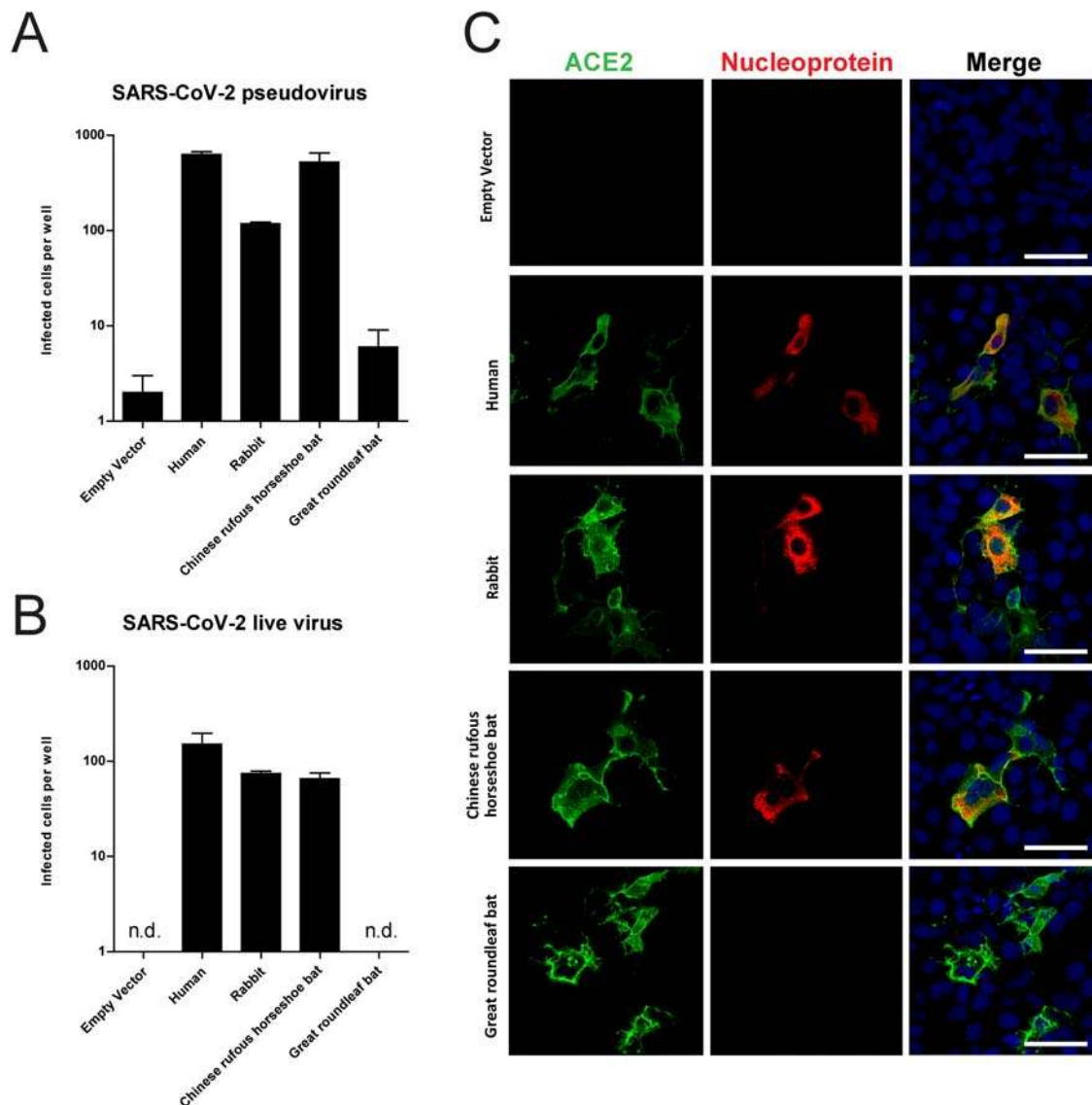


Figure 1. Rabbit ACE2-mediated SARS-CoV-2 infection. SARS-CoV-2 pseudovirus (A) and authentic virus (B) infection of Cos-7 cells transfected with ACE2 of various species. Infectivity was quantified by staining live virus with anti-SARS-CoV nucleocapsid and scanning live virus and pseudovirus infected cells. (C) Confocal imaging of ACE2-mediated live virus infection; cells were stained using anti-human ACE2 in green, anti-SARS-CoV nucleocapsid in red and TO-PRO3 in blue to stain nuclei. Scale indicates 50 μ m. n.d. = not detected. Error bars depict SEM.

5.13), 14, 11 and 9 days p.i. per animal in the throat (mean shedding of 11.33 days, $SD = 2.52$) and 9, 4 and 2 days p.i. per animal in the rectum (mean shedding of 5 days, $SD = 3.61$). Infectious virus shedding from the nose lasted for 6, 7 and 7 days p.i. per animal (mean shedding of 6.67 days, $SD = 0.58$) with a peak at day two for all three animals, followed by a second peak at day seven for two animals (Figure 2(B)). In the throat, infectious virus was detected only on day one p.i. for one animal. No infectious virus was detected in rectal swabs. All animals followed up to day 21 seroconverted with plaque reduction neutralization test ($PRNT_{50}$) titres of 1:40, 1:320 and 1:640.

Additionally, three groups of three animals were inoculated with either 10^4 , 10^5 or 10^6 $TCID_{50}$ SARS-CoV-2 and swabs were taken for four days before the animals were euthanized and necropsied.

All animals inoculated with 10^6 $TCID_{50}$ were viral RNA positive in the nose and throat for at least four days with a single animal positive in the rectum at day three (Figure 2(C)). Animals inoculated with 10^5 $TCID_{50}$ were RNA positive in the nose for at least four days, for at least three days in the throat but not in the rectum (Figure 2(D)). Two of these animals also shed infectious virus in the nose for three days and two days respectively (mean shedding of 1.67 days, $SD = 1.53$) and one animal shed virus two days post infection in the throat (Supplementary Figure 1). Animals inoculated with 10^4 $TCID_{50}$ did not shed any detectable viral RNA (Figure 2(E)). Although nasal turbinates yielded on average 8.42×10^3 RNA copies/mL, lung homogenates of animals inoculated with 10^6 $TCID_{50}$ virus were found viral RNA negative (Figure 2(F)). Despite the fact

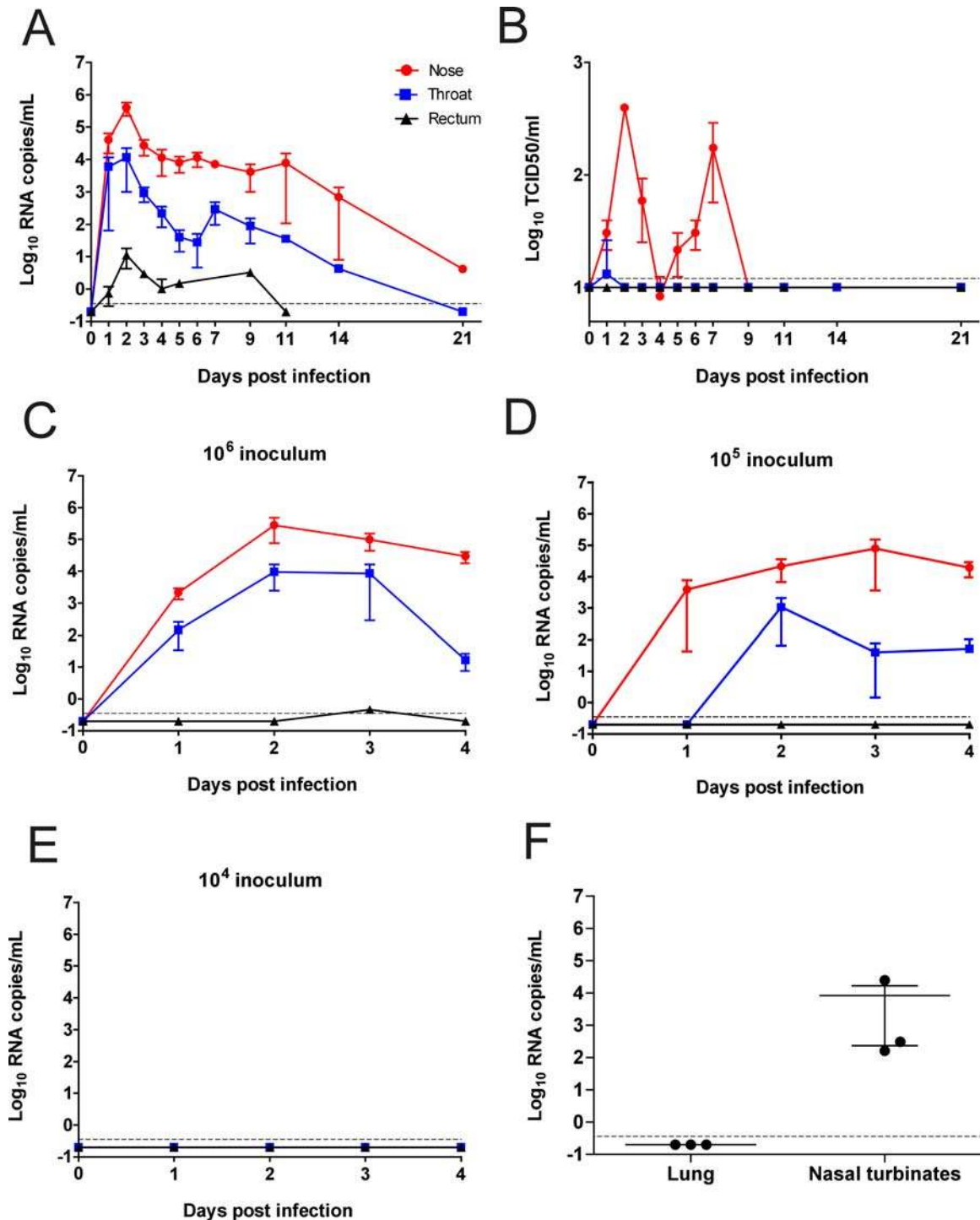


Figure 2. Susceptibility of rabbits to SARS-CoV-2 infection. Infection kinetics of (A) viral RNA and (B) authentic SARS-CoV-2 virus growth curves from rabbits inoculated with 10^6 TCID₅₀ and followed up for 21 days. (C–E) Viral RNA growth curves in rabbits inoculated with either (C) 10^6 , (D) 10^5 , or (E) 10^4 TCID₅₀ and followed up for four days post infection. (F) Viral RNA in lung and nasal turbinates of 10^6 TCID₅₀ infected rabbits, sacrificed after four days. The RNA detection limit was 3.5×10^{-1} RNA copies/mL, while the live virus detection limit is 12.5 TCID₅₀/mL. Error bars depict SEM. $n = 3$.

that no viral RNA was detected in the lungs, histological examination of the lungs of infected animals sacrificed four days p.i. revealed a multifocal mild to moderate increase in alveolar macrophages in the alveolar lumina with multifocal presence of few neutrophils. Mainly associated with the terminal bronchioles, multifocal mild thickening of the septa, with infiltrations of neutrophils, eosinophils

and occasional lymphocytes, plasma cells and macrophages were observed (Figure 3(A)). Mild multifocal necrosis of alveolar epithelial cells and the presence of a few enlarged, syncytial cells in the alveolar lumina were seen (Figure 3(B)). There was mild peribronchiolar and peribronchial lymphoplasmacytic infiltration with eosinophils and moderate to severe bronchus-associated lymphoid tissue proliferation

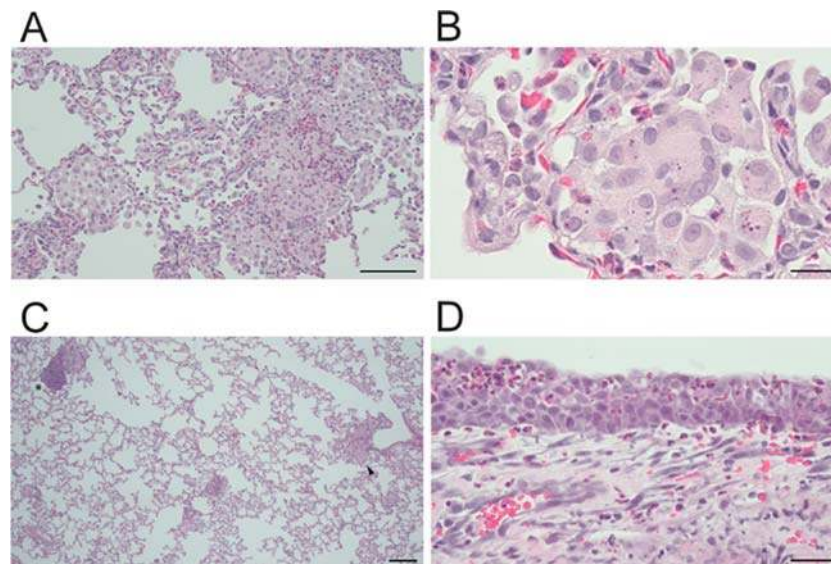


Figure 3. Histological analysis of SARS-CoV-2 infected rabbits. Histopathological analysis of rabbits inoculated with 10^6 TCID₅₀, sacrificed after four days. (A) Alveolar thickening and inflammatory infiltrates. Scale indicates 100 μ m (B) Enlarged, syncytial cells in the alveolar lumina. Scale indicates 20 μ m. (C) Lung pathology overview. Arrow indicates thickening and asterisk bronchus-associated lymphoid tissue (BALT). Scale indicates 200 μ m. (D) Eosinophilic infiltrates in the nose. Scale indicates 40 μ m.

(Figure 3(C)). Some animals showed enlarged tracheo-bronchial lymph nodes consistent with mild lymphoid hyperplasia. In the nose, there was multifocal infiltration of moderate numbers of eosinophils and lymphoplasmacytic infiltrates in the olfactory epithelium (exocytosis) and in the lamina propria, alongside mild hyperplasia and hypertrophy of the olfactory epithelium (Figure 3(D)). Mild eosinophilic exocytosis was present in the trachea. Although lung pathology was observed, no antigen was present in immunohistochemistry stainings of lung or nose tissue.

Discussion

This study demonstrates that rabbits are susceptible to SARS-CoV-2. While the infection is asymptomatic, infectious virus with peak titres corresponding to $\sim 10^3$ TCID₅₀ could be detected up to day seven post inoculation in the nose. The minimum dose to establish productive infection was 10^5 TCID₅₀, indicating that virus transmission between rabbits may be less efficient compared to ferrets and hamsters. The use of young, immunocompetent, and healthy New Zealand White rabbits in this study however may not reflect virus shedding and disease in other rabbit breeds or rabbits at different ages. Thus, surveillance studies – including serological testing – may be needed to assess the presence of SARS-CoV-2 in farmed rabbits.

Viral shedding in rabbits occurred in a biphasic pattern, which was also observed for SARS-CoV-2 infected African green monkeys [16]. This pattern is potentially linked to early innate immune responses that act within days, followed by adaptive

responses that generally take one week to be activated. These observations are in line with recent findings that the presence of neutralizing serum antibodies in humans negatively correlates with infectious virus shedding, and that shedding of viral RNA outlasts shedding of infectious virus [17]. The presence of eosinophils in the nose and lungs of infected animals suggests a possible helper T cell 2 (Th2)-mediated immune response. The preferential upper respiratory tract infection in the absence of robust replication in the lower respiratory tract of rabbits resembles what has been observed in experimentally inoculated ferrets [7].

The transmission of SARS-CoV-2 to mink caused viral spread between farm animals and spill-over to humans, resulting in mass culling of mink to limit the spread of the virus [8]. Circulation of the virus in high density captivity could cause the virus to adapt to lagomorphs, increasing the risk of intraspecies transmission between farmed and possibly wild lagomorphs. This study provides evidence of susceptibility of rabbits to SARS-CoV-2 infection warranting further investigations on the presence of SARS-CoV-2 in lagomorphs.

Acknowledgements

This research is partly financed by the Netherlands Organization for Health Research and Development (ZONMW) grant agreement 10150062010008 to B.L.H and co-funded by the PPP Allowance (grant agreement LSHM19136) made available by Health Holland, Top Sector Life Sciences & Health, to stimulate public-private partnerships. This manuscript was part of the research programme of the Netherlands Centre for One Health (www.ncohl.nl).

Disclosure statement

No potential conflict of interest was reported by the author(s).

Funding

This work was supported by Netherlands Organization for Health Research and Development [grant number 10150062010008]; PPP Allowance [grant number LSHM19136].

ORCID

Anna Z. Mykytyn  <http://orcid.org/0000-0001-7188-6871>

Mart M. Lamers  <http://orcid.org/0000-0002-1431-4022>

Nisreen M. A. Okba  <http://orcid.org/0000-0002-2394-1079>

Tim I. Breugem  <http://orcid.org/0000-0002-5558-7043>

Debby Schipper  <http://orcid.org/0000-0001-6449-4765>


Petra B. van den Doel  <http://orcid.org/0000-0002-5735-5537>

Peter van Run  <http://orcid.org/0000-0001-6963-4165>

Leon de Waal  <http://orcid.org/0000-0002-7596-7270>

Marion P. G. Koopmans  <http://orcid.org/0000-0002-5204-2312>

Koert J. Stittelaar  <http://orcid.org/0000-0002-0607-3214>

Judith M. A. van den Brand  <http://orcid.org/0000-0001-8420-5406>

Bart L. Haagmans  <http://orcid.org/0000-0001-6221-2015>

References

- World Health Organization. Coronavirus disease (COVID-19) pandemic. 2020. Available from: <https://www.who.int/emergencies/diseases/novel-coronavirus-2019>.
- Chan JF, Zhang AJ, Yuan S, et al. Simulation of the clinical and pathological manifestations of Coronavirus Disease 2019 (COVID-19) in golden Syrian hamster model: implications for disease pathogenesis and transmissibility. *Clin Infect Dis*. 2020 Mar 26. doi:10.1093/cid/ciaa325. PubMed PMID: 32215622; PubMed Central PMCID: PMC7184405.
- Rockx B, Kuiken T, Herfst S, et al. Comparative pathogenesis of COVID-19, MERS, and SARS in a nonhuman primate model. *Science*. 2020 May 29;368(6494):1012–1015. doi:10.1126/science.abb7314. PubMed PMID: 32303590; PubMed Central PMCID: PMC7164679.
- Sia SF, Yan LM, Chin AWH, et al. Pathogenesis and transmission of SARS-CoV-2 in golden hamsters. *Nature*. 2020 May 14. doi:10.1038/s41586-020-2342-5. PubMed PMID: 32408338.
- Fagre A, Lewis J, Eckley M, et al. SARS-CoV-2 infection, neuropathogenesis and transmission among deer mice: Implications for reverse zoonosis to New World rodents. *bioRxiv*. 2020 Aug 7. doi:10.1101/2020.08.07.241810. PubMed PMID: 32793912; PubMed Central PMCID: PMC7418741. eng.
- Griffin BD, Chan M, Taylor N, et al. North American deer mice are susceptible to SARS-CoV-2. *bioRxiv*. 2020:2020.07.25. doi:10.1101/2020.07.25.221291.
- Shi J, Wen Z, Zhong G, et al. Susceptibility of ferrets, cats, dogs, and other domesticated animals to SARS-coronavirus 2. *Science*. 2020: eabb7015, doi:10.1126/science.abb7015.
- Oreshkova N, Molenaar RJ, Vreman S, et al. SARS-CoV-2 infection in farmed minks, the Netherlands, April and May 2020. *Euro Surveill*. 2020 Jun;25(23). doi:10.2807/1560-7917.ES.2020.25.23.2001005. PubMed PMID: 32553059; eng.
- Whelan SP, Ball LA, Barr JN, et al. Efficient recovery of infectious vesicular stomatitis virus entirely from cDNA clones. *Proc Natl Acad Sci U S A*. 1995 Aug 29;92(18):8388–8392. doi:10.1073/pnas.92.18.8388. PubMed PMID: 7667300; PubMed Central PMCID: PMC7173433; eng.
- Hierholzer JC, Killington RA. Virus isolation and quantitation. *Virology Methods Manual*. 1996: 25–46. doi:10.1016/b978-012465330-6/50003-8. PubMed PMID: PMC7173433; eng.
- Okba NMA, Muller MA, Li W, et al. Severe acute respiratory syndrome coronavirus 2-specific antibody responses in coronavirus disease Patients. *Emerg Infect Dis*. 2020 Jul;26(7):1478–1488. doi:10.3201/eid2607.200841. PubMed PMID: 32267220; PubMed Central PMCID: PMC7323511. eng.
- Corman VM, Landt O, Kaiser M, et al. Detection of 2019 novel coronavirus (2019-nCoV) by real-time RT-PCR [published correction appears in *Euro Surveill*. 2020 Apr;25(14):] [published correction appears in *Euro Surveill*. 2020 Jul;25(30):]. *Euro Surveill*. 2020;25(3):2000045. doi:10.2807/1560-7917.ES.2020.25.3.2000045
- Haagmans BL, Kuiken T, Martina BE, et al. Pegylated interferon-alpha protects type I pneumocytes against SARS coronavirus infection in macaques. *Nat Med*. 2004 Mar;10(3):290–293. doi:10.1038/nm1001. PubMed PMID: 14981511; PubMed Central PMCID: PMC7095986.
- Zhou P, Yang XL, Wang XG, et al. A pneumonia outbreak associated with a new coronavirus of probable bat origin. *Nature*. 2020 Mar;579(7798):270–273. doi:10.1038/s41586-020-2012-7. PubMed PMID: 32015507; PubMed Central PMCID: PMC7095418.
- Li F. Structure, Function, and Evolution of coronavirus spike Proteins. *Annu Rev Virol*. 2016 Sep 29;3(1):237–261. doi:10.1146/annurev-virology-110615-042301. PubMed PMID: 27578435; PubMed Central PMCID: PMC7095418.
- Zhao X, Chen D, Szabla R, et al. Broad and differential animal ACE2 receptor usage by SARS-CoV-2. *J Virol*. 2020 Jul 13. doi:10.1128/JVI.00940-20. PubMed PMID: 32661139.
- Hartman AL, Nambulli S, McMillen CM, et al. SARS-CoV-2 infection of African green monkeys results in mild respiratory disease discernible by PET/CT imaging and shedding of infectious virus from both respiratory and gastrointestinal tracts. *PLoS Pathog*. 2020 Sep;16(9):e1008903, doi:10.1371/journal.ppat.1008903PPATHOGENS-D-20-01799. [pii]. PubMed PMID: 32946524; PubMed Central PMCID: PMC7535860. eng.
- van Kampen JJA, van de Vijver DAMC, Fraaij PLA, et al. Shedding of infectious virus in hospitalized patients with coronavirus disease-2019 (COVID-19): duration and key determinants. *medRxiv*. 2020:2020.06.08. doi:10.1101/2020.06.08.20125310.